Chien-Kuo Wang, MD
Chun-Wei Li, PhD
Tsyh-Jyi Hsieh, MD
Sang-Hsiung Chien, MD
Gin-Chung Liu, MD
Kun-Bow Tsai, MD

Index terms:
Bone neoplasms, 40.31, 40.32, 40.33, 40.35, 40.37
Bone neoplasms, MR, 40.121411, 40.121413, 40.121415, 40.12143, 40.12145
Magnetic resonance (MR), spectroscopy, 40.121415, 40.12145
Soft tissues, MR, 40.121411, 40.121413, 40.121415, 40.12143, 40.12145
Soft tissues, neoplasms, 40.36, 40.37, 40.39

Published online
10.1148/radiol.2322031441
Radiology 2004; 232:599–605

[1] From the Departments of Medical Imaging (C.K.W., T.J.H., G.C.L.), Orthopedics (S.H.C.), and Pathology (K.B.T.), Chung-Ho Memorial Hospital and Faculty of Medical Radiation Technology (C.W.L.), Kaohsiung Medical University, 100 Tzyou 1st Rd, Kaohsiung 807, Taiwan. From the 2003 RSNA scientific assembly. Received September 9, 2003; revision requested November 20; revision received November 27; accepted January 19, 2004. **Address correspondence to** C.K.W. (e-mail: *wangck@kmu.edu.tw*).

Author contributions:
Guarantors of integrity of entire study, C.K.W., C.W.L., G.C.L.; study concepts, C.K.W., C.W.L.; study design, C.K.W.; literature research, C.K.W., T.J.H.; clinical studies, C.K.W., T.J.H., S.H.C.; data acquisition, C.K.W., C.W.L., K.B.T.; data analysis/interpretation, C.K.W., C.W.L.; statistical analysis, C.K.W.; manuscript preparation, C.K.W.; manuscript definition of intellectual content, C.K.W., C.W.L.; manuscript editing, C.W.L., G.C.L.; manuscript revision/review, C.K.W., G.C.L.; manuscript final version approval, C.K.W., C.W.L., G.C.L.

Characterization of Bone and Soft-Tissue Tumors with in Vivo ^{1}H MR Spectroscopy: Initial Results[1]

PURPOSE: To determine if in vivo detection of choline by using hydrogen 1 (^{1}H) magnetic resonance (MR) spectroscopy with dynamic contrast material–enhanced MR imaging can help differentiate between benign and malignant musculoskeletal tumors.

MATERIALS AND METHODS: MR imaging was performed in 36 consecutive patients with bone and soft-tissue tumors larger than 1.5 cm in diameter. Examinations were performed at 1.5 T with a surface coil appropriate for the location of the lesions. Single-voxel ^{1}H MR spectroscopy was performed by using a point-resolved spectroscopic sequence with echo times of 40, 135, and 270 msec. The volume of interest within lesions was positioned on the areas of early enhancement (<8 seconds after arterial enhancement) according to the findings of dynamic contrast-enhanced MR imaging with subtraction. The criterion for determining whether choline was present in a lesion was a clearly identifiable peak at 3.2 ppm in at least two of the three spectra acquired at echo times. MR spectroscopic results and histopathologic findings were determined in blinded fashion and compared with κ statistics. $P < .001$ was considered to indicate a significant difference.

RESULTS: Choline was detected in 18 of 19 patients with malignant tumors and in three of 17 patients with benign lesions. The three benign lesions included one perineurioma, one giant cell tumor, and one abscess. Choline was not detected in 14 patients with benign lesions nor in one patient with a densely ossifying low-grade parosteal osteosarcoma. In vivo ^{1}H MR spectroscopy characterized bone and soft-tissue tumors, resulting in a sensitivity of 95%, specificity of 82%, and accuracy of 89% ($P < .001$).

CONCLUSION: Choline can be reliably detected in large malignant bone and soft-tissue tumors by using a multiecho point-resolved spectroscopic protocol. ^{1}H MR spectroscopy can help differentiate malignant from benign musculoskeletal tumors by revealing the presence or absence of water-soluble choline metabolites.

The effectiveness of magnetic resonance (MR) imaging in accurate characterization of musculoskeletal tumors has not gone unquestioned (1–9). Improvement in the treatment and outcome of patients with bone and soft-tissue tumors requires the development of diagnostic tools that can help differentiate between benign and malignant lesions in a noninvasive and reliable manner. During the past few years, differentiation between benign and malignant masses on unenhanced MR images has been based mainly on the evaluation of morphologic parameters such as size, demarcation of margins, involvement of adjacent vital structures, signal homogeneity, and measurements of relaxation times (2,6,7,10,11). In dynamic gradient-echo MR studies, this technique provides clinically useful information by depicting tissue vascularization and perfusion, capillary permeability, and composition of interstitial space (5,12). Attempts have been made to use the slope of a time-intensity curve, which reflects the increased signal intensity after the adminis-

tration of a contrast agent, as a criterion for differentiation between benign (low-slope) and malignant (high-slope) lesions (1,4,5,9,13,14).

Despite the highly statistically significant differences in slope values between benign and malignant lesions, sensitivity and specificity are adversely affected by slope values of poorly vascularized malignant tumors and highly vascularized benign tumors, such as giant cell tumor, granulation tissue, capillary or arteriovenous hemangioma, and abscess (4,5). Authors of a study have suggested that the enhancement parameters used for dynamic contrast material–enhanced MR imaging, such as start of enhancement, enhancement patterns, and progression of enhancement, could be used to improve the sensitivity in differential diagnosis of soft-tissue masses (9). However, because of the overlap between benign and malignant lesions, time-intensity curves and slope values should be used only in combination with conventional spin-echo images and other radiologic, anatomic, and clinical data to narrow down the differential diagnostic possibilities (12).

In addition to imaging features, information regarding the cellular chemistry obtainable from ex vivo or in vitro hydrogen 1 (^{1}H) nuclear MR spectroscopy (15–19) may help characterize suspicious lesions. Reports have demonstrated that the composition of membrane phospholipid in tumor tissue is an important indicator of a tumor's cellularity, proliferative capacity, and differentiation state. Millis et al (16) have reported that the phosphatidylcholine level on ex vivo nuclear MR spectra as an estimate of the total tissue cell membrane phospholipid mass in pleomorphic liposarcoma was three times higher than that in dedifferentiated liposarcoma. The pleomorphic liposarcoma is the most aggressive and metastatic subtype of liposarcoma. Mukherji et al (18) also reported that the choline-creatine ratio obtained by in vitro ^{1}H MR spectroscopy was capable of helping to distinguish malignant tumors of the extracranial head and neck from the uninvolved muscle. The choline-creatine ratio is markedly higher in squamous cell carcinoma than in muscle. In vivo ^{1}H MR spectroscopy has been utilized for analysis of bone and soft-tissue tumors (20), as well as other malignant lesions (21), such as breast carcinoma (22–24), prostate cancer (25), and cervical carcinoma (26). The preliminary study of in vivo ^{1}H MR spectroscopy in bone and soft-tissue tumors by Oya et al (20) did not focus on the level of choline-containing compounds at 3.2 ppm. However, the malignancies in breast, prostate, and cervix peaked at a chemical shift of 3.2 ppm, which corresponded to that of choline at ^{1}H MR spectroscopy (22–26).

Detection of choline with absolute measurement methods (27) requires an external standard because neither fat nor water can serve as an internal reference. If an external standard is placed near the lesions, variations in signal amplitude measurements and the reference due to magnetic field inhomogeneities may lead to ambiguous concentration estimates (28). Yeung et al (23) reported that a multiecho acquisition approach for determining the presence or absence of choline at in vivo ^{1}H MR spectroscopy is a useful tool in the characterization of breast lesions. Because well-vascularized viable areas of a tumor can be identified with dynamic contrast-enhanced MR imaging, which provides physiologic information about the vascularization and perfusion of the lesion, the correct positioning of the volume of interest for suspicious lesions during ^{1}H MR spectroscopy can be guided by the use of dynamic contrast-enhanced MR images.

The aim of the present study was to determine if in vivo detection of choline by using ^{1}H MR spectroscopy performed with dynamic contrast-enhanced MR imaging can help differentiate between benign and malignant musculoskeletal tumors.

MATERIALS AND METHODS

Patients

Thirty-six patients (mean age, 47.8 years; age range, 13–87 years) with bone and soft-tissue tumors larger than 1.5 cm in diameter were included in the study. There were 16 male (mean age, 49.9 years ± 18.5; range, 18–87 years) and 20 female (mean age, 46.1 years ± 18.7; range, 13–70) patients. The patients were enrolled consecutively between November 2002 and May 2003. The study was approved by our institutional medical ethical review board. Informed consent was obtained from all patients prior to examination. MR examinations were included in our routine protocol for the evaluation of the tumor extent and to obtain baseline information for possible neoadjuvant chemotherapy. No interventional procedures such as biopsy or aspiration were performed on the tumors prior to MR studies.

MR Imaging and MR Spectroscopy

The examinations were performed with a 1.5-T whole-body MR imaging system (Gyroscan ACS-NT; Philips, Best, the Netherlands). A body coil was used for identification of tumors. An appropriate surface coil was selected for MR spectroscopy. Transverse and sagittal or coronal images were obtained by using a T1-weighted spin-echo sequence (500/14 [repetition time msec/echo time msec], two signals acquired, 512 × 512 matrix size, section thickness and intersection gap depending on tumor size) and a T2-weighted turbo spin-echo sequence with fat suppression (1,800/160/100 [repetition time msec/echo time msec/inversion time msec], three signals acquired, 512 × 512 matrix size, section thickness and intersection gap depending on tumor size). After a bolus of 0.1 mmol per kilogram of body weight gadopentetate dimeglumine (Magnevist; Schering, Berlin, Germany) was intravenously injected with an MR-compatible power injector (Spectris; Medrad, Pittsburgh, Pa) at 2 mL/sec, dynamic contrast-enhanced MR images covering the entire lesions were acquired by using a T1-weighted turbo-field-echo sequence (15/4.1, 25° flip angle, one signal acquired, 256 × 256 matrix size, section thickness and intersection gap variable). Each phase was no longer than 8 seconds. The dynamic imaging time lasted 3 minutes after intravenous administration of contrast material. Image subtraction was then performed to show areas of early enhancement on the subtracted images. The delayed contrast-enhanced transverse and sagittal or coronal images were obtained by using T1-weighted spin-echo spectral presaturation with inversion recovery sequence (500/14, two signals acquired, 512 × 512 matrix size, section thickness and intersection gap variable).

Spectra for each volume of interest were acquired 10–15 minutes after the administration of contrast material by using the point-resolved spectroscopic sequence (2,000/40, 2,000/135, and 2,000/270). A staff musculoskeletal radiologist (H.T.J.) with 4 years of experience carefully positioned one volume of interest (mean volume, 6.2 cm^3; range, 3.4–21 cm^3) to include the early enhancing areas of the tumors, as demonstrated on the subtracted images. Inclusion of the adjacent bone cortex and muscle was avoided. If a slowly enhancing tumor or absence of enhancement during the 3-minute acquisition was depicted, the volume of interest fitted the size of tu-

Summary of MR Spectroscopic and Pathologic Findings

Patient No./ Age(y)/Sex	Tumor Location	Tumor Size in Long Axis (cm)	Pathologic Finding	Voxel Size (cm^3)	Choline Signal		
					40-msec TE	135-msec TE	270-msec TE
1/17/F	Vastus medialis	4.43	Hemangioma	8.0	No	No	No
2/65/F	Thigh	3.18	Nodular fasciitis	5.6	Yes	No	No
3/65/F	Gluteus maximus	11.8	Lymphoma	21.0	Yes	Yes	Yes
4/50/M	Hand	2.75	Trichilemmal cyst	3.4	No	No	No
5/68/F	Femur	2.43	Metastasis	3.4	Yes	Yes	Yes
6/25/M	Fibula	12.87	Osteosarcoma	6.6	Yes	Yes	Yes
7/55/M	Elbow	5.55	Hematoma	8.6	Yes	No	No
8/56/M	Leg	2.95	Ganglion	3.4	No	No	No
9/70/M	Inguinal area	5.15	Metastasis	6.8	No*	Yes	Yes
10/32/M	Femur	10.39	Fibrous dysplasia	5.2	No	No	No
11/58/F	Gluteal region	4.18	Bursitis	4.2	No	No	No
12/45/F	Inguinal area	3.30	Lymphoma	4.6	Yes	Yes	Yes
13/13/F	Arm	3.37	Pilomatricoma	4.9	No	No	No
14/66/F	Arm	4.50	Lipoma	6.8	No	No	No
15/54/M	Knee	7.62	Tuberculous arthritis	3.4	No	No	No
16/25/F	Femur	11.05	Parosteal osteosarcoma	4.1	No	No	No
17/54/F	Sacrum	5.87	Metastasis	8.0	Yes	Yes	Yes
18/44/F	Foot	3.94	Perineurioma	4.0	Yes	Yes	Yes
19/46/M	Vastus lateralis	3.20	Foreign body granuloma	3.4	No	No	No
20/29/F	Wrist	3.64	GCT of tendon sheath	3.4	No	No	No
21/32/M	Thigh	3.98	Metastasis	4.5	Yes	Yes	No
22/47/M	Femur	5.91	GCT	4.2	No	No	No
23/39/M	Tibia	6.16	Metastasis	4.1	Yes	Yes	Yes
24/56/F	Pelvis	7.09	Metastasis	9.3	Yes	Yes	Yes
25/56/F	Ilium	6.87	Metastasis	5.2	Yes	Yes	Yes
26/64/F	Fibula	10.74	Osteosarcoma	5.8	Yes	Yes	Yes
27/37/F	Thigh	4.02	Hemangioma	6.9	No	No	No
28/48/M	Femur	7.75	Metastasis	6.3	Yes	Yes	Yes
29/22/F	Femur	5.19	GCT	7.5	Yes	Yes	No
30/66/M	Pelvic sidewall	6.84	Leiomyosarcoma	9.6	Yes	Yes	Yes
31/27/F	Thigh	14.26	Abscess	8.4	Yes	Yes	Yes
32/87/M	Sacrum	2.80	Metastasis	3.6	Yes	Yes	Yes
33/70/F	Pelvis	6.26	Metastasis	4.5	Yes	Yes	No
34/41/F	Thigh	3.54	Liposarcoma	4.1	Yes	Yes	Yes
35/18/M	Arm	11.41	Epitheloid sarcoma	9.5	Yes	Yes	Yes
36/74/M	Sacrum	8.19	Metastasis	12.3	Yes	Yes	No

Note.—GCT = giant cell tumor, TE = echo time.
* Prominent resonances derived from fatty acids masked the choline peak at 3.2 ppm.

mors according to the delayed contrast-enhanced MR images. Automated optimization of transmitter pulse power, localized shimming, gradient tuning, and water suppression were used. The parameters used to perform MR spectroscopy were a spectral width of 1,000 Hz and 128 signals acquired, and the time required to complete the examination was approximately 20 minutes.

After acquisition, MR spectroscopic data were processed by a physicist (L.C.W.) with 15 years of experience with MR spectroscopy. The commercial MR software package provided by the manufacture was used. In the time domain, spectrum processing parameters are zero filled to 2,048 data points, 3-Hz Gaussian line-broadening filter, phase correction, and baseline correction. The criterion for determining whether choline was present in a lesion was the presence of a clearly identifiable peak at 3.2 ppm in at least two of the three spectra acquired at different echo times.

Histopathologic diagnoses of bone and soft-tissue tumors were established with resected specimens in 24 patients, specimens from core biopsy with a 16-gauge needle (Temno Biopsy System; Allegiance, Tokyo, Japan) in nine patients, and specimens from core biopsy with a bone marrow biopsy needle (Trap System; MD Tech, Gainesville, Fla) in three patients. Histopathologic examinations of the samples were performed by one pathologist (T.K.P.) with 7 years of experience with musculoskeletal tumors. The tumor cell differentiation, necrosis, and mitosis were evaluated. Both the radiologist and the pathologist were blinded to the MR spectroscopic measurements performed by the physicist.

Statistical Analysis

The age between the male and female groups was evaluated by using a two-sample t test. $P < .05$ was considered to indicate a statistically significant difference.

The κ statistic was used to compare MR spectroscopic results with histopathologic and surgical information. The resultant data were analyzed with software (SPSS, version 10.0; SPSS, Chicago, Ill). A κ value of 0.40 or less was considered to indicate marginal reproducibility; 0.40–0.75, good reproducibility; and 0.75–1.00, excellent reproducibility. $P < .001$ was considered to indicate a statistically significant difference. True-positive, true-negative, false-positive, and false-negative detection rates, as well as sensitivity and specificity, were determined.

RESULTS

Tumor Types

There was no significant difference between the mean age of the male and female groups ($P > .05$). Nineteen patients

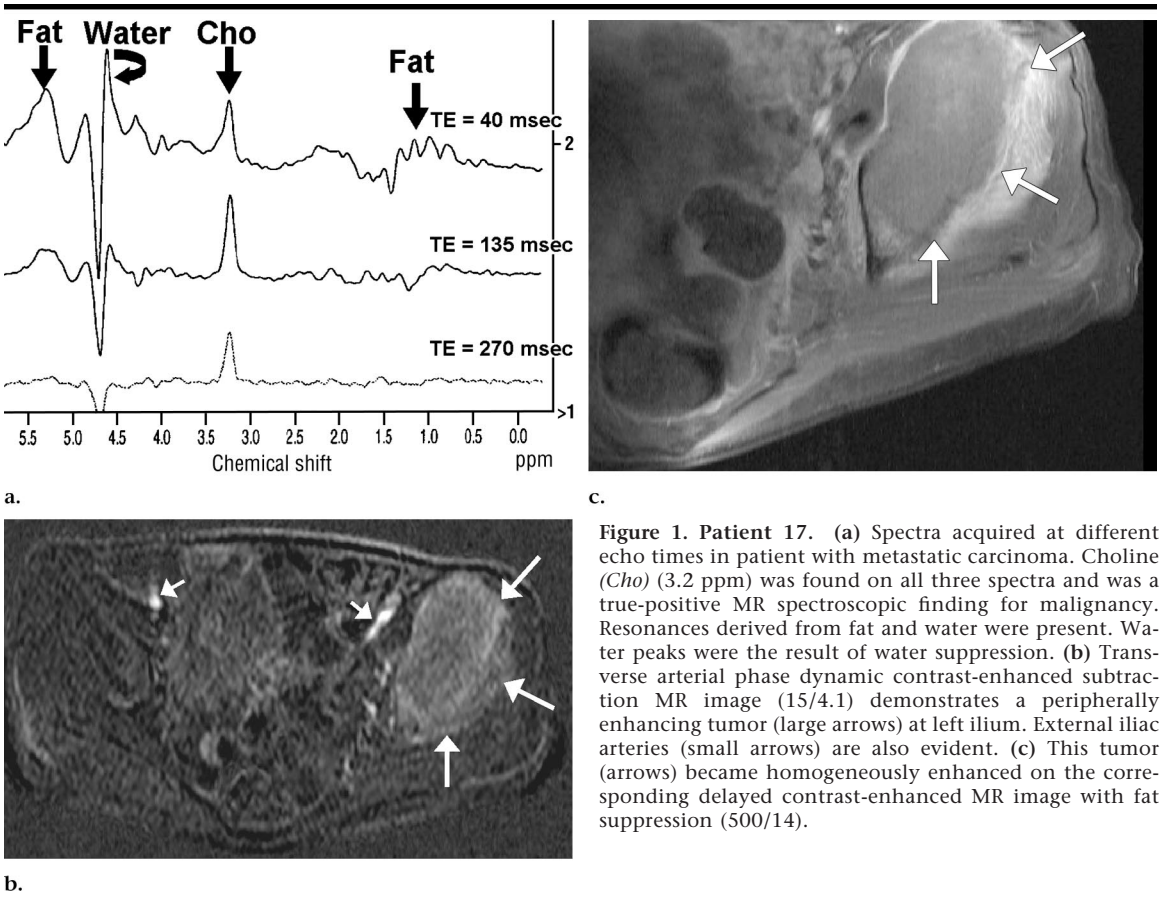

Figure 1. Patient 17. **(a)** Spectra acquired at different echo times in patient with metastatic carcinoma. Choline *(Cho)* (3.2 ppm) was found on all three spectra and was a true-positive MR spectroscopic finding for malignancy. Resonances derived from fat and water were present. Water peaks were the result of water suppression. **(b)** Transverse arterial phase dynamic contrast-enhanced subtraction MR image (15/4.1) demonstrates a peripherally enhancing tumor (large arrows) at left ilium. External iliac arteries (small arrows) are also evident. **(c)** This tumor (arrows) became homogeneously enhanced on the corresponding delayed contrast-enhanced MR image with fat suppression (500/14).

had malignant bone and soft-tissue tumors, including 11 metastatic tumors, three osteosarcomas, two lymphomas, one leiomyosarcoma, one liposarcoma, and one epitheloid sarcoma. The mean size of these tumors was 7.06 cm (range, 2.43–12.87 cm). Seventeen patients had benign lesions, including two soft-tissue hemangiomas, two giant cell tumors, one nodular fasciitis, one trichilemmal cyst, one hematoma, one ganglion, one fibrous dysplasia, one case of bursitis, one pilomatricoma, one lipoma, one case of tuberculous arthritis, one perineurioma, one foreign body granuloma, one giant cell tumor of tendon sheath, and one abscess. The mean size of these lesions was 5.24 cm (range, 2.75–14.26 cm).

MR Spectroscopy

The Table summarizes the MR spectroscopic and histopathologic findings of the musculoskeletal lesions in all 36 patients. In 18 patients with malignant tumors, a resonance at 3.2 ppm attributed to a choline-containing compound was detected (Fig 1). In 14 of the 17 patients with benign lesions, no choline signal was detected. Choline was found in three benign lesions, including one perineurioma (patient 18), one giant cell tumor (patient 29), and one abscess (patient 31). The peaks in 3.2-ppm regions were detected on the spectra, with all three echo times in the perineurioma (Fig 2) and abscess. The spectra of the patient with giant cell tumor were positive, with echo times of 40 and 135 msec. Choline was not detected in one malignant parosteal osteosarcoma (patient 16) (Fig 3). Seventeen of 21 positive choline findings were based on spectra with all three echo times; the remaining four positive findings, on spectra with two echo times. Thirteen of the 15 negative choline findings were determined on the basis of the absence of any identifiable signal in the 3.2-ppm region above the baseline noise on spectra obtained with all three echo times, and only peaks at 3.2 ppm with an echo time of 40 msec were found in the remaining two negative cases (patients 2 and 7). Signal contribution arising from fat in the 0.9–2.1 and 5.3-ppm regions decreased with increasing echo time, which resulted in an improved spectral resolution. However, with an increasing echo time, a decreasing spectral signal-to-noise ratio was observed due to relaxation losses.

Overall, the true-positive detection rate of malignant bone and soft-tissue lesions was 18 of 19; the true-negative rate, 14 of 17; the false-positive rate, three of 17; and the false-negative rate, one of 19. Therefore, in vivo ^{1}H MR spectroscopy had a sensitivity of 95% (18 of 19), specificity of 82% (14 of 17), positive predictive value of 86% (18 of 21), negative predictive value of 93% (14 of 15), and accuracy of 89% (32 of 36). Excellent agreement between MR spectroscopic and histopathologic findings was present, as indicated by the κ value of 0.776 ± 0.105 ($P < .001$).

DISCUSSION

Using a multiecho acquisition approach to determine the presence or absence of choline in bone and soft-tissue tumors in vivo, we found a strong relationship between ^{1}H MR spectroscopic and histopathologic findings. The position of

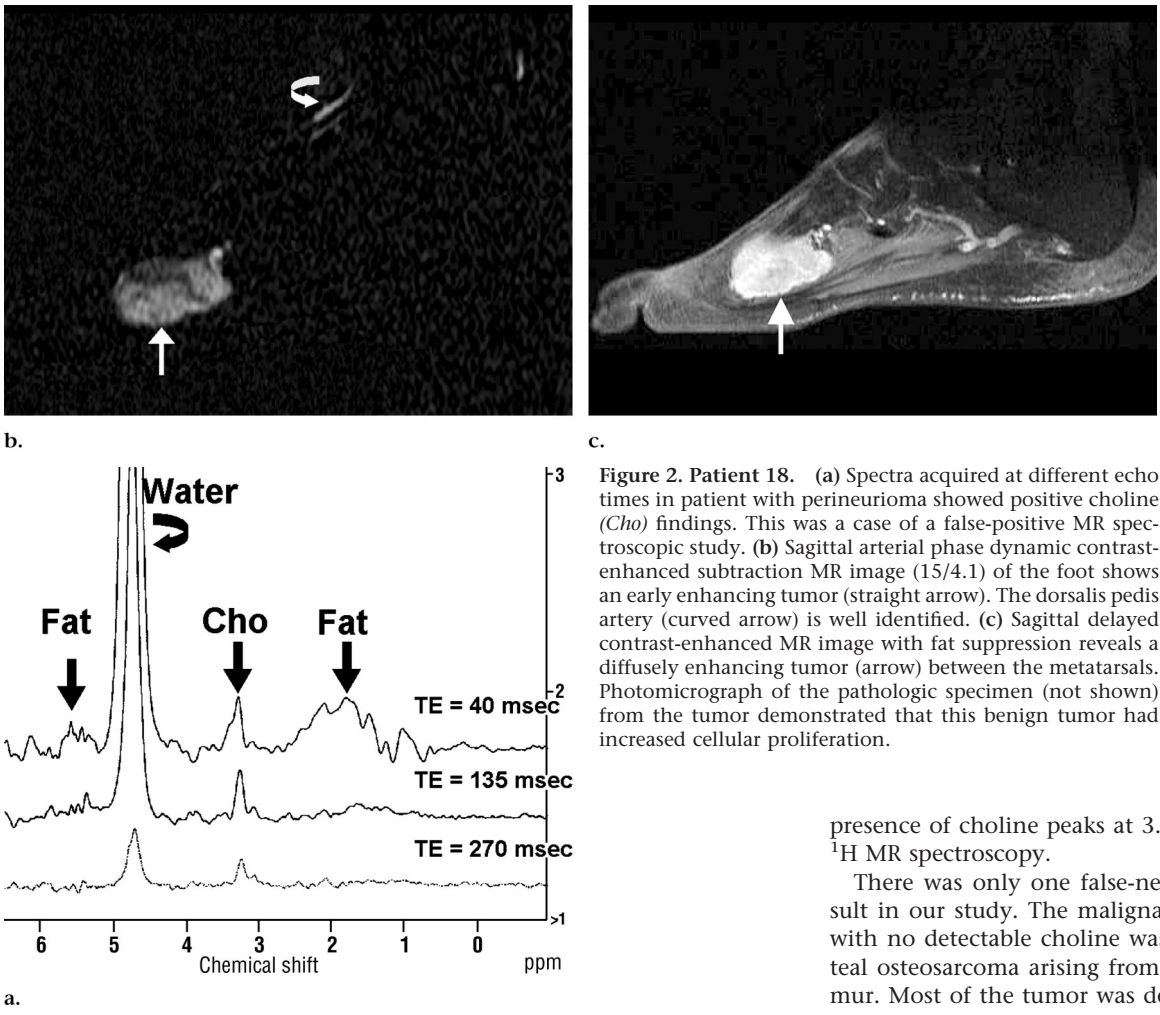

Figure 2. Patient 18. **(a)** Spectra acquired at different echo times in patient with perineurioma showed positive choline *(Cho)* findings. This was a case of a false-positive MR spectroscopic study. **(b)** Sagittal arterial phase dynamic contrast-enhanced subtraction MR image (15/4.1) of the foot shows an early enhancing tumor (straight arrow). The dorsalis pedis artery (curved arrow) is well identified. **(c)** Sagittal delayed contrast-enhanced MR image with fat suppression reveals a diffusely enhancing tumor (arrow) between the metatarsals. Photomicrograph of the pathologic specimen (not shown) from the tumor demonstrated that this benign tumor had increased cellular proliferation.

the volume of interest, including the early enhanced regions inside the lesions, is determined with dynamic contrast-enhanced images. According to van der Woude et al (9), the early enhanced regions represent areas of high biologic activities, such as cellularity, cell turnover time, and neovascularity. In malignant tumors, these areas may contain more choline-containing compounds. A 15% decrease in the choline signal was noted after injection of contrast material during chemical shift imaging with a long echo time (29). However, authors of single-voxel ^{1}H MR spectroscopic studies (30,31) have found no statistically significant differences in long- or short-echo-time acquisitions following the administration of contrast material.

Three of the 17 benign lesions found in our patients were false-positive. These lesions included one perineurioma, one giant cell tumor, and one abscess. The histologic findings of perineurioma, as well as of giant cell tumor, showed hypercellularity and hypervascularity. The pathologic examination of the patient with abscess demonstrated an abundance of inflammatory cells in the wall of abscess. Choline and its derivatives are thought to represent important constituents in the phospholipid metabolism of cell membranes (32). In vivo, the choline peak (resonance at 3.2 ppm) is composed of choline, phosphocholine, phosphatidylcholine, and glycerophosphocholine. Elevation of this peak is thought to represent increased membrane phospholipid biosynthesis and also to be an active marker for cellular proliferation (21,33). Previous reports have demonstrated that benign tumors that are hypercellular may show an elevated choline level in brain lesions, as well as in head and neck tumors (34–36). In addition, a large number of inflammation-related cells produced by inflammatory processes may also result in a high choline peak (37). The cellular proliferation and/or cell density of these lesions may explain the presence of choline peaks at 3.2 ppm in ^{1}H MR spectroscopy.

There was only one false-negative result in our study. The malignant tumor with no detectable choline was a parosteal osteosarcoma arising from distal femur. Most of the tumor was densely ossified. Prevention of ossification in the volume of interest was impossible. The lower proton amounts and susceptibility effects due to mineralization may account for the false-negative choline uptake in this case. Another possible explanation is the low-grade malignancy of this kind of tumor. The parosteal osteosarcoma has a better prognosis than do other subtypes of osteosarcoma.

In vitro ^{1}H MR spectroscopy of the normal muscle can show two peaks with almost the same height at 3.0 and 3.2 ppm (38). The volume of interest should be positioned carefully inside the tumor. In our study, most cases had no identifiable signal at 3.0 ppm that was attributed to a creatine-containing compound. Therefore, the contamination from the adjacent muscle that causes the choline signal at 3.2 ppm can be eliminated.

A limitation of this study was the exclusion of smaller lesions (<1.5 cm in diameter). In vivo ^{1}H MR spectroscopy with a 1.5-T MR imager is not possible with a voxel size of less than 1 cm^3. The decreased signal-to-noise ratio in the

smaller voxel also makes interpretation of spectra difficult. The 3.0-T MR imager may increase signal-to-noise ratio and can acquire reliable spectra from smaller lesions.

There were very diverse pathologic conditions in this study, which included a variety of metastases, primary malignant and benign bone tumors, and a number of nonneoplastic lesions. With these limited numbers, it is difficult to draw meaningful conclusions regarding a specific disease. Another limitation of the study was the total, relatively small, number of tumors imaged. Further studies focusing on a specific disease should be performed in a larger group of patients.

In conclusion, our results demonstrate that choline can be detected in contrast-enhanced bone and soft-tissue tumors or tumorlike lesions in vivo by using a multiecho point-resolved spectroscopic sequence. In the evaluation of 36 patients for bone and soft-tissue tumors based on the presence of choline, the sensitivity, specificity, and accuracy of ^{1}H MR spectroscopy were 95%, 82%, and 89%, respectively. The information provided with ^{1}H MR spectroscopy and dynamic contrast-enhanced MR imaging may complement other findings, such as adjacent bone invasion and tissue plane destruction, and may improve the diagnostic specificity of MR examination in the identification of malignancy.

Acknowledgments: Special thanks to Yuan-Yu Chiau, RT, and Feng-O Shu, RT, for MR technical assistance and Faline Lin and Chu-Hui Min for preparation of this manuscript.

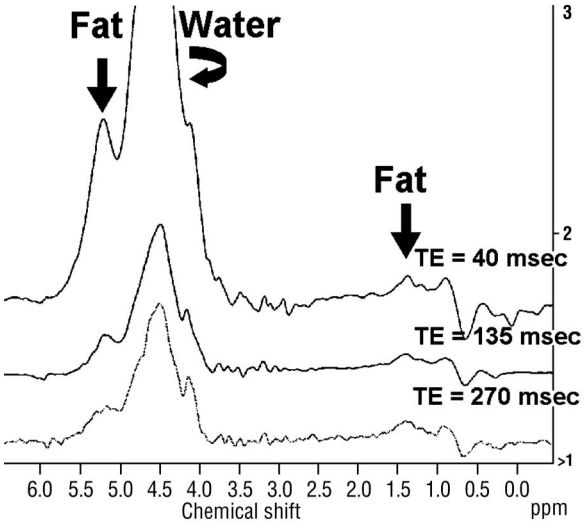

a.

b.

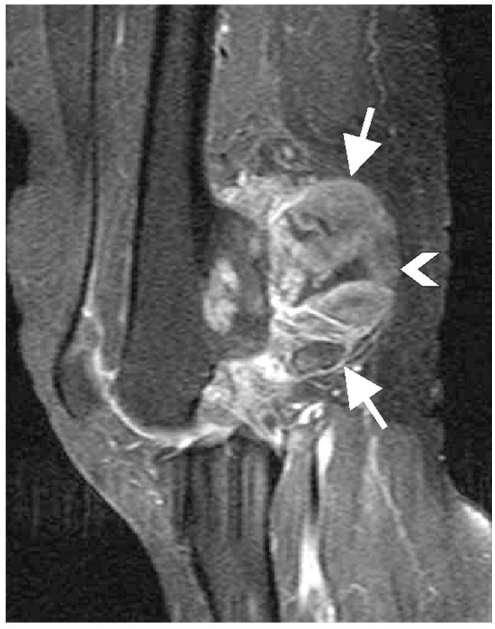

c.

Figure 3. Patient 16. **(a)** False-negative spectra acquired at different echo times in patient with intensely ossified parosteal osteosarcoma showed no choline resonance above the baseline noise at 3.2 ppm. **(b)** Sagittal arterial phase dynamic contrast-enhanced subtraction MR image (15/4.1) of the knee shows a tumor with heterogeneous enhancement from periphery (arrows). **(c)** Sagittal delayed contrast-enhanced MR image with fat suppression (500/14) depicts central unenhanced cleft (arrowhead) within the enhancing tumor (arrows) from the posterior periosteum of distal femur.

References

1. Erlemann R, Reiser MF, Peters PE, et al. Musculoskeletal neoplasms: static and dynamic Gd-DTPA-enhanced MR imaging. Radiology 1989; 171:767–773.
2. Berquist TH, Ehman RL, King BF, Hodgman CG, Ilstrup DM. Value of MR imaging in differentiating benign from malignant soft-tissue masses: study of 95 lesions. AJR Am J Roentgenol 1990; 155: 1251–1255.
3. Mirowitz SA, Totty WG, Lee JK. Characterization of musculoskeletal masses using dynamic Gd-DTPA enhanced spin-echo MRI. J Comput Assist Tomogr 1992; 16:120–125.
4. Verstraete KL, Dierick A, De Deene Y, et al. First-pass images of musculoskeletal lesions: a new and useful diagnostic application of dynamic contrast-enhanced MRI. Magn Reson Imaging 1994; 12:687–702.
5. Verstraete KL, De Deene Y, Roels H, Dierick A, Uyttendaele D, Kunnen M. Benign and malignant musculoskeletal lesions: dynamic contrast-enhanced MR imaging—parametric "first-pass" images depict tissue vascularization and perfusion. Radiology 1994; 192:835–843.
6. Totty WG, Murphy WA, Lee JK. Soft-tissue tumors: MR imaging. Radiology 1986; 160:135–141.
7. Crim JR, Seeger LL, Yao L, Chandnani V, Eckardt JJ. Diagnosis of soft-tissue masses with MR imaging: can benign masses be differentiated from malignant ones? Radiology 1992; 185:581–586.
8. May DA, Good RB, Smith DK, Parsons TW. MR imaging of musculoskeletal tumors and tumor mimickers with intravenous gadolinium: experience with 242 patients. Skeletal Radiol 1997; 26:2–15.
9. van der Woude HJ, Verstraete KL, Hogendoorn PC, Taminiau AH, Hermans J, Bloem JL. Musculoskeletal tumors: does fast dynamic contrast-enhanced subtraction MR imaging contribute to the characterization? Radiology 1998; 208:821–828.
10. Sundaram M, McGuire MH, Schajowicz F. Soft-tissue masses: histologic basis for decreased signal (short T2) on T2-weighted

images. AJR Am J Roentgenol 1987; 148: 1247–1250.
11. Pettersson H, Slone RM, Spanier S, Gillespy T 3rd, Fitzsimmons JR, Scott KN. Musculoskeletal tumors: T1 and T2 relaxation times. Radiology 1988; 167:783–785.
12. Verstraete KL, van der Woude HJ. Dynamic contrast-enhanced magnetic resonance imaging. In: De Schepper AM, ed. Imaging of soft tissue tumors. 2nd ed. Berlin, Germany: Springer-Verlag, 2001; 83–104.
13. Fletcher BD, Reddick WE, Taylor JS. Dynamic MR imaging of musculoskeletal neoplasms. Radiology 1996; 200:869–872.
14. Verstraete KL, van der Woude HJ, Hogendoorn PC, De Deene Y, Kunnen M, Bloem JL. Dynamic contrast-enhanced MRI in the musculoskeletal system. J Magn Reson Imaging 1996; 6:311–321.
15. Smith IC, Blandford DE. Diagnosis of cancer in humans by 1H NMR of tissue biopsies. Biochem Cell Biol 1998; 76:472–476.
16. Millis K, Weybright P, Campbell N, et al. Classification of human liposarcoma and lipoma using ex vivo proton NMR spectroscopy. Magn Reson Med 1999; 41:257–267.
17. Singer S. New diagnostic modalities in soft tissue sarcoma. Semin Surg Oncol 1999; 17:11–22.
18. Mukherji SK, Schiro S, Castillo M, et al. Proton MR spectroscopy of squamous cell carcinoma of the upper aerodigestive tract: in vitro characteristics. AJNR Am J Neuroradiol 1996; 17:1485–1490.
19. Mackinnon WB, Barry PA, Malycha PL, et al. Fine-needle biopsy specimens of benign breast lesions distinguished from invasive cancer ex vivo with proton MR spectroscopy. Radiology 1997; 204:661–666.
20. Oya N, Aoki J, Shinozaki T, et al. Preliminary study of proton magnetic resonance spectroscopy in bone and soft tissue tumors: an unassigned signal at 2.0–2.1 ppm may be a possible indicator of malignant neuroectodermal tumor. Radiat Med 2000; 18:193–198.
21. Negendank W. Studies of human tumors by MRS: a review. NMR Biomed 1992; 5:303–324.
22. Kvistad KA, Bakken IJ, Gribbestad IS, et al. Characterization of neoplastic and normal human breast tissues with in vivo (1)H MR spectroscopy. J Magn Reson Imaging 1999; 10:159–164.
23. Yeung DK, Cheung HS, Tse GM. Human breast lesions: characterization with contrast-enhanced in vivo proton MR spectroscopy—initial results. Radiology 2001; 220:40–46.
24. Gribbestad IS, Singstad TE, Nilsen G, et al. In vivo (1)H MRS of normal breast and breast tumors using a dedicated double breast coil. J Magn Reson Imaging 1998; 8:1191–1197.
25. Kurhanewicz J, Vigneron DB, Hricak H, et al. Three-dimensional H-1 MR spectroscopic imaging of the in situ human prostate with high (0.24–0.7-cm^3) spatial resolution. Radiology 1996; 198:795–805.
26. Allen JR, Prost RW, Griffith OW, et al. In vivo proton (H1) magnetic resonance spectroscopy for cervical carcinoma. Am J Clin Oncol 2001; 24:522–529.
27. Gribbestad IS, Bakken IJ, Singstad TE, Kvistad KA. Determination of choline content in breast tumors with H-1 MR spectroscopy: an external standard method (abstr). In: Proceedings of the Seventh Meeting of the International Society for Magnetic Resonance in Medicine. Berkeley, Calif: International Society for Magnetic Resonance in Medicine, 1999; 1587.
28. Christiansen P, Henriksen O, Stubgaard M, Gideon P, Larsson HB. In vivo quantification of brain metabolites by 1H-MRS using water as an internal standard. Magn Reson Imaging 1993; 11:107–118.
29. Sijens PE, van den Bent MJ, Nowak PJ, van Dijk P, Oudkerk M. 1H chemical shift imaging reveals loss of brain tumor choline signal after administration of Gd-contrast. Magn Reson Med 1997; 37:222–225.
30. Taylor JS, Reddick WE, Kingsley PB, Ogg RJ. Proton MRS after gadolinium contrast agent (abstr). In: Proceedings of the Society of Magnetic Resonance in Medicine and the European Society of Magnetic Resonance in Medicine and Biology. Berkeley, Calif: Society of Magnetic Resonance in Medicine, 1995; 1854.
31. Lin A, Ross BD. The effect of gadolinium on quantitative short-echo time single voxel MRS of treated and untreated brain tumors (abstr). In: Proceedings of the Eighth Meeting of the International Society for Magnetic Resonance in Medicine. Berkeley, Calif: International Society for Magnetic Resonance in Medicine, 1999; 390.
32. Miller BL. A review of chemical issues in 1-H NMR spectroscopy: n-acetyl-L-aspartate, creatine and choline. NMR Biomed 1991; 4:47–52.
33. Ruiz-Cabello J, Cohen JS. Phospholipid metabolites as indicators of cancer cell function. NMR Biomed 1992; 5:226–233.
34. Rand SD, Prost R, Haughton V, et al. Accuracy of single voxel proton MR spectroscopy in distinguishing neoplastic from nonneoplastic brain lesions. AJNR Am J Neuroradiol 1997; 18:1695–1704.
35. Krouwer HG, Kim TA, Rand SD, et al. Single voxel proton MR spectroscopy of nonneoplastic brain lesions suggestive of a neoplasm. AJNR Am J Neuroradiol 1998; 19:1695–1703.
36. Maheshwari SR, Mukherji SK, Neelon B, et al. The choline/creatine ratio in five benign neoplasms: comparison with squamous cell carcinoma by use of in vitro MR spectroscopy. AJNR Am J Neuroradiol 2000; 21:1930–1935.
37. Bitsch A, Bruhn H, Vougioukas V, et al. Inflammatory CNS demyelination: histopathologic correlation with in vivo quantitative proton spectroscopy. AJNR Am J Neuroradiol 1999; 20:1619–1627.
38. Sharma U, Atri S, Sharma MC, Sarkar C, Jagannathan NR. Skeletal muscle metabolism in Duchenne muscular dystrophy (DMD): an in-vitro proton NMR spectroscopy study. Magn Reson Imaging 2003; 21:145–153.